Modelling river dune splitting

C.M. Dohmen-Janssen, J. Lansink, A.J. Paarlberg & S.J.M.H. Hulscher
University of Twente, Department of Water Engineering and Management, PO Box 217, 7500 AE Enschede, the Netherlands, phone: +31-53-489 4209, fax: +31-53-489 5377, email: c.m.dohmen-janssen@utwente.nl

A.P.P. Termes
HKV Consultants, Lelystad, the Netherlands

ABSTRACT: The dune development model of Paarlberg et al. (2006; subm.) is able to predict evolution of dune height from small initial bed disturbances to equilibrium dimensions reasonably well with limited computational time. However, dune length is largely overestimated, because of continuous merging of dunes, while dune splitting does not occur in the model. The current paper presents a method to include dune splitting in this model. Based on a literature study and new laboratory experiments performed at the University of Auckland, New Zealand, we implement dune splitting by superposition of TRIAS-ripples (i.e. TRIangular Asymmetric Stoss side-ripples) on the stoss sides of developing dunes as soon as these stoss sides exceed a certain critical length. This critical length is determined from a stability analysis as the smallest wave length that can grow. Results of the extended model show that predictions of dune characteristics are significantly improved, compared to the original model.

1 INTRODUCTION

River dunes are rhythmic patterns that develop on the river bed due to the interaction between the turbulent flow and the sandy bottom. They have heights in the order of 10 - 30% of the water depth and lengths in the order of 10 times their heights, they migrate in downstream direction and are of asymmetrical shape with mild stoss sides slopes and steep lee sides, often reaching the angle of repose (about 30°). For steep lee sides, a flow separation zone develops behind the dune in which flow near the bottom is reversed due to the recirculating eddy that develops in this zone. During floods, river dunes grow and decay as a result of the changing flow conditions and influence water levels significantly, because they act as roughness to the flow. Accurate forecasts of water levels during floods therefore require accurate predictions of the evolution of river dune dimensions.

In the past, many different approaches have been followed to model dune dimensions, varying from equilibrium dune height predictors (e.g. Yalin 1964, Allen 1978, Van Rijn 1984) to different forms of stability analyses (e.g. Kennedy 1963, Engelund 1970, Fredsøe 1974, Yamaguchi & Izumi 2002). Recently, models have been developed that calculate in detail the turbulent flow field over bed forms, in some cases in combination with morphological computations (e.g. Shimizu et al. 2001, Nelson et al. 2005, Tjerry & Fredsoe 2005, Giri & Shimizu 2006). These models are very valuable to study detailed hydrodynamic processes, but are extremely computationally intensive, which is partly due to the complexity of calculating the turbulent flow in the flow separation zone behind the leeside of the dunes.

To predict evolution of dune dimensions over the time-scale of a discharge wave, computation time should be limited. To that end we developed a dune evolution model in which the flow and sediment transport at the flow separation zone is modeled in a parameterized way (Paarlberg et al. 2006; subm.). This model is able to predict the evolution of dunes from small initial disturbances up to equilibrium dimensions with limited computational time. If the dune length in the model is fixed at the fastest growing mode (found from the stability analysis embedded in the model), the dune height predicted by the model is in good agreement with measurements.

However, if the dune length is allowed to vary, it keeps on growing until one long dune occupies the complete model domain. Because the increase in dune length is accompanied by an increase in dune height, both dune length and dune height are overestimated by the model in this case. The continuous growth of dunes is probably caused by the fact that dune merging is included in the model, but dune splitting is not. Both in the model and in reality dunes merge due to the fact that dunes of different dimensions have different migration velocities. The

faster migrating dunes therefore catch up with the slower ones and finally merge, leading to longer dunes (see e.g. Leclair 2002). However, in reality dunes have also been observed to break up (split), thereby reducing the dune length (see e.g. Jerolmack and Mohrig 2005). Dune splitting does not occur in the Paarlberg model.

The objective of the present study is to improve predictions of dune evolution by implementing the process of dune splitting in the Paarlberg model. This has lead to the following research questions:

1 What is the mechanism behind dune splitting that results in limited growth of dune length?
2 How can dune splitting be implemented in the Paarlberg model and does this lead to better predictions of dune dimensions?

To answer the first question we performed new laboratory experiments at the University of Auckland, New Zealand, in addition to evaluating existing knowledge about the splitting mechanism from literature. We used this knowledge to implement dune splitting in the Paarlberg model. The dune development model of Paarlberg et al. (2006; subm.) is briefly presented in Section 2. Section 3 describes the experiments that were carried out to study the dune splitting mechanism. In Section 4 we explain in which way we implemented the splitting mechanism in the dune development model. Validation of the extended dune development model is presented in Section 5. Results are discussed in Section 6 and Section 7 presents the main conclusions of this study.

2 DUNE DEVELOPMENT MODEL

2.1 *General set-up of the model*

The dune development model of Paarlberg et al. (2006; subm.), consists of a flow module, a sediment transport module and a bed evolution module. Flow and bed morphology are solved in a decoupled manner. Flow separation and sediment transport in the flow separation zone are included in a parameterized way.

2.2 *Flow module*

The flow module consists of the 2DV-hydrostatic shallow water equations. As a basic turbulence closure, a constant eddy viscosity is used in combination with a partial slip condition at the bed.

When dunes grow, they get more asymmetrical and eventually the lee side becomes so steep that the flow separates behind the dune crest. In the Paarlberg model, the flow inside the flow separation zone is not modeled. Instead, a parameterization of the separation streamline is determined (see Paarlberg et al. 2007), which is used as an artificial bed over which the flow is calculated.

2.3 *Sediment transport and bed evolution modules*

Only bed load sediment transport is included in the model. A Meyer-Peter Muller type bed load formulation is applied, which includes bed slope effects and uses the turbulence-averaged shear stresses from the flow module as input. The bed slope effects included in the model represent the fact that sediment is easier set in motion on a downhill slope than on an uphill slope (slope effect on critical shear stress) and the fact that sediment moves easier downhill than uphill (slope effect on actual shear stress). The bed evolution module consists of the Exner-equation which is based on sediment continuity and describes the fact that bed evolution is a result of convergences and divergences in sediment transport.

Sediment transport rates in the flow separation zone, and between the reattachment point and the dune crest, are parameterized. At the flow separation point it is assumed that all sediment passing over the dune crest avalanches down the lee side and deposits evenly over the lee side at the angle of repose. At the flow reattachment point, the turbulence-averaged shear stress and thus the sediment transport rate are assumed to be zero. Next, the shear stress over the stoss side (between the reattachment point and the dune crest) is parameterized, such that it gradually increases from zero at the reattachment to the maximum value at the dune crest, as calculated by the flow module. This parameterized shear stress is used to calculate the sediment transport rate over the stoss side, its gradients and the resulting bed evolution.

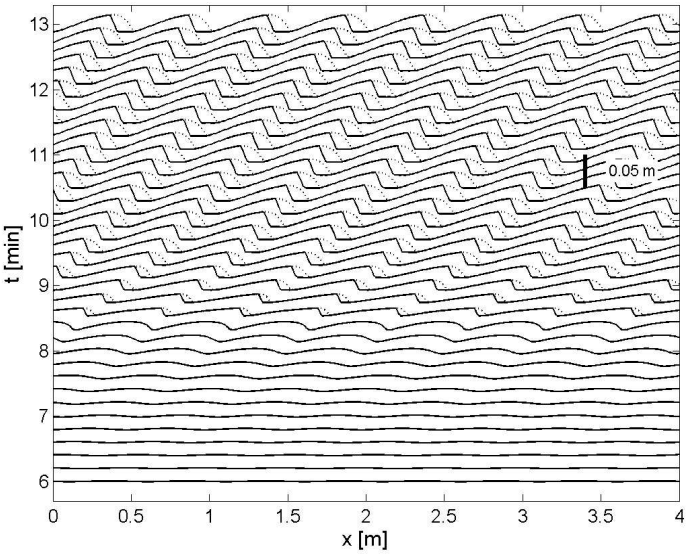

Figure 1. Dune development calculated by the Paarlberg model for laboratory conditions using fixed dune length resulting from linear stability analysis (flow is from left to right).

2.4 *Model results of dune development and merging*

As an example, Figure 1 presents a typical result of the Paarlberg model for laboratory conditions, as a stacked plot of bed profiles. Every line in this plot shows a calculated bottom profile as a function of the distance along the flume with a time spacing of 12 *s*. It shows dune evolution from small sinusoidal initial disturbances with a wave length based on linear stability analysis. Dashed lines present parameterizations of separation streamlines.

If a random disturbance is applied to an initially flat bed, dunes of different wave lengths and different migration velocities are formed. As a result, slower dunes are caught up by faster migrating dunes and the two dunes merge, as observed in reality. However, splitting of individual bed forms into smaller features is not observed in the model (see Fig. 2).

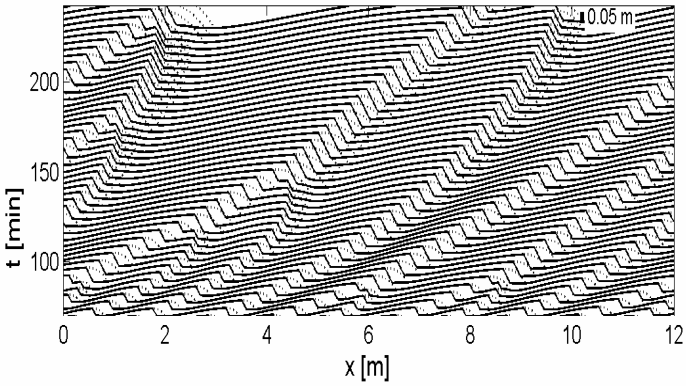

Figure 2. Simulated dune evolution (from 50 - 250 *min* after the start of the simulation), resulting from a randomly disturbed bed, showing merging of dunes.

3 LABORATORY EXPERIMENTS

3.1 *Experimental set-up*

The aim of the experiments was to observe how dunes split during their development and in equilibrium conditions and to formulate potential mechanisms responsible for dune splitting that can be implemented in the Paarlberg dune development model. Thereto, experiments have been carried out in a laboratory flume at the University of Auckland, New Zealand, in which dune development processes can be studied in detail (see also Friedrich et al., 2007).

The glass-sided flume is 12 *m* long and 0.44 *m* wide. Both water and sediment are recirculated and the flume can be tilted. The flume was filled with a 60 *mm* thick layer of sediment with a median grain size D_{50} = 0.85 *mm*. The D_{10} (10% finest grain size) and D_{90} (10% coarsest grain size) are about 0.6 and 1.1 *mm*, respectively.

3.2 *Measuring techniques*

Flow velocities were measured at the start of each experiment (when the bed was still flat) using an Acoustic Doppler Velocimeter (ADV). The measurements were taken at the downstream end of the flume at several heights above the sand bed.

Centreline bed profiles were measured over a 6 *m* long test section located between 4 and 10 *m* from the sand and water inlet. Measurements were made using an automatic carriage system, which consists of a depth sounding probe and a potentiometer that measures the position of the carriage along the flume. Bed elevations were recorded roughly every 23 *s* (i.e. one entire bed profile every 23 *s)*. The horizontal spacing is approximately 2.5 *mm*. According to Coleman & Melville (1997) the accuracy of the bed elevation measurements is ± 0.4 *mm*.

Dune evolution during the course of an experiment is recorded by a fixed video camera over a section of 1.5 *m*. A handheld camera was used to observe small-scale processes.

3.3 *Experimental conditions*

Three steady flow conditions were selected, all with the same flume width b and bed slope i_0, but different specific discharges q and initial water level depths H_0 (see Table 1). Table 1 also presents the equilibrium water depth (after dune formation) H_{eq}, the mean flow velocity U and the Froude number Fr (see Sections 3.4 and 3.5 for further explanation of these parameters).

Table 1. Experimental conditions.

Test	b	i_0	q	H_0	H_{eq}	U	Fr
	m	-	m^2/s	*m*	*m*	*m/s*	-
T22	0.44	0.0015	0.0994	0.150	0.19	0.65	0.54
T23	0.44	0.0015	0.0817	0.125	0.16	0.62	0.56
T24	0.44	0.0015	0.0618	0.100	0.13	0.58	0.58

3.4 *Experimental procedure*

After distributing the sand evenly over the flume, the flume was carefully filled with water to the initial water depth (H_0). The bed was flattened before each run to make sure that all experiments started with the same initial bottom configuration. To obtain the desired bed slope, the flume was tilted. Water temperature, initial water level and bed slope were recorded before the start of an experiment.

At t = 0, the pumps (sediment and water) were turned on, simultaneously with the start of the bed profile measurement. During the experiments, the water surface slope was kept parallel to the bed slope by adjusting a tail gate when a discrepancy was observed.

3.5 *Post-processing of the data*

Depth-averaged mean flow velocities U were estimated by fitting a logarithmic profile through the ADV-data and finding the velocity at $1/e$ of the height of the water column above the sand bed. The mean velocity U was used to calculate the Froude number $Fr = U/\sqrt{(gH_0)}$.

Dune height Δ, dune length λ and dune aspect ratio Δ/λ were derived from the profile measurements using the tool *Bedformer*. This tool requires a threshold dune height, which is set at 10 mm to filter out local random bed-level variations of only a few grain diameters and small ripples.

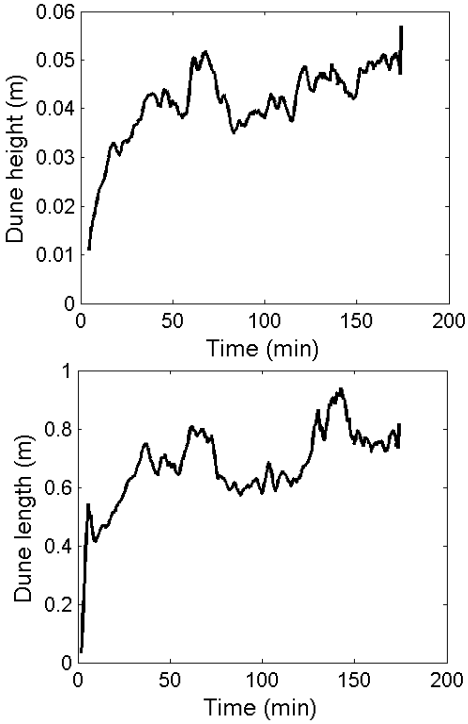

Figure 3. Evolution of dune height (upper panel) and dune length (lower panel) during the course of experiment T22.

3.6 *Experimental results – general dune evolution*

For the three experimental conditions, the evolution of dune height, dune length and dune aspect ratio during the course of the experiment was derived from the bed profile measurements. As an example, the results for test T22 are presented in Figure 3. This figure shows that initially, dune dimensions increase rapidly. After a certain time, dune dimensions do not change anymore and are considered to have reached the equilibrium stage. The observed equilibrium dune height Δ_{eq}, dune length λ_{eq} and dune aspect ratio $(\Delta/\lambda)_{eq}$ are presented in Table 2 for all three experiments.

Table 2. Experimental results – equilibrium dune dimensions.

Test	Δ_{eq} *m*	λ_{eq} *m*	$(\Delta/\lambda)_{eq}$ -
T22	0.050	0.75	0.066
T23	0.044	0.70	0.066
T24	0.036	0.70	0.051

3.7 *Experimental results - dune splitting*

During the experiments, we observed pile-ups of sediment, superimposed on stoss sides. These pile-ups are probably caused by turbulent bursting and can develop into small dunes and develop a lee side.

As an example, Figure 4 shows a stacked plot of bed profiles (time spacing = 1 *min*). This figure shows the presence of a large dune with an angle of repose lee side and a long and gentle stoss side (I). Because of the long stoss side, it acts as a flat bed and we see several attempts of small bed forms developing on the stoss side. Most of them are washed away. The ones that generate a real leeside (II & III) migrate faster than the underlying dune (I).

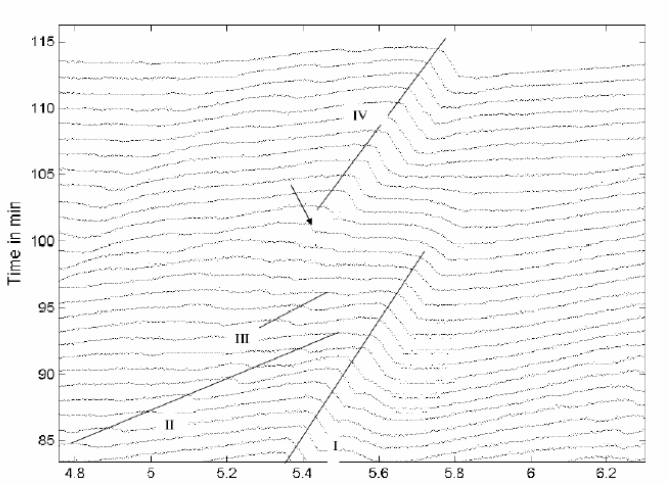

Figure 4. Measured bed profiles (time spacing = 1 *min*) as a function of the distance along the measurement section.

At the arrow in Fig.4, we see a different behaviour: the lee side of this small bed form is so steep that flow separation occurs, which causes sediment to stop migrating downstream and initiates the growth of dune IV. Dune I is cut off of sediment. This shows that relatively high and steep superimposed bed forms decrease the stoss side length of long dunes. The random initiation of small superimposed bed forms seems one of the main mechanisms for dune splitting.

Superimposed bed features are observed in numerous flume and field experiments. An extensive reference is given by Venditti et al. (2005). They give a detailed description of, what they call, sand sheets, which have heights of about 10% of the height of the underlying dune, migration velocities of about 8 - 10 times the dune migration rate, nearly constant lengths and aspect ratios of approximately 1:40.

These superimposed features develop a certain distance downstream of the flow reattachment point, which is linked to the regrowing internal boundary layer and increasing shear stress. Directly downstream of the flow reattachment point the turbulence-averaged bed shear stress does not exceed the threshold for sediment movement. Further downstream, the internal boundary layer regrows, in the

same way as the boundary over a flat bed develops. Therefore, a long stoss side acts like a flat bed and new dunes are generated in a similar way as initiation from a flat bed.

Development of the sand sheets observed by Venditti et al. (2005) appeared also to be related to a minimum distance from the crest of the upstream dune. They found that if the underlying dune has a wavelength in the range 0.5–1 *m*, superposition occurs on the stoss side of dunes over a length of about three times the separation zone length at a distance of at least 0.5 *m* from the crest of the upstream dune.

4 IMPLEMENTATION OF DUNE SPLITTING

4.1 *Imposing a small random disturbance*

Since we observed in the experiments that random initiation of small superimposed bed forms seems one of the main mechanisms for dune splitting, we tried to implement this in the Paarlberg dune development model. In the model, dune initiation does not occur on a perfectly flat bed, but is triggered by irregularities in the bed profile, such as the random pile ups of grains (probably related to turbulence bursts) observed in the measurements. However, due to model simplifications, random pile ups of grains or turbulence bursts do not occur in the model simulations. Therefore, we have introduced a random disturbance signal every 10^{th} time step, to mimic the influence of turbulent flow structures on the bed.

The random signal is applied under the condition that no flow separation was present to avoid numerical difficulties in determining the parameterized bed over a disturbed bed. The maximum value of this disturbance was set to two grain diameters ($2D_{50}$). The spacing (Δx) has the same value as the grid size of the calculation (i.e. $\Delta x = 0.01$ *m*). The disturbance is added every 10^{th} time step. If we would increase the frequency of the disturbance (e.g. every time step) dune development depends too strong on the disturbance. The bed then becomes an accumulation of disturbances instead of an outcome of the model equations. Figure 5 shows a stacked plot of bed profiles from model simulations in which a random disturbance is introduced every 10^{th} time step. It shows a strong diffusion of the applied disturbance and shows that growth of the applied disturbance or scouring of the underlying dune is not perceived.

To investigate the diffusive behaviour of the random disturbance, we performed a nonlinear stability analysis to determine which superimposed disturbances are able to grow on the developed dunes. Results of this stability analysis are presented in Figure 6, which shows negative growth rates for superimposed bed features with wavelengths smaller than about 0.5 *m*. This explains why the small random disturbances are quickly damped by the model and implies that the method of adding small random disturbances will not lead to initiation of dune splitting.

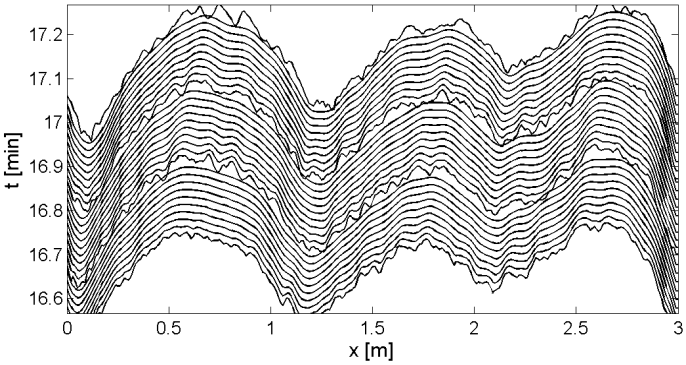

Figure 5. Calculated bed profiles at each time step (= 1 s), with a random small disturbance added every 10th time step.

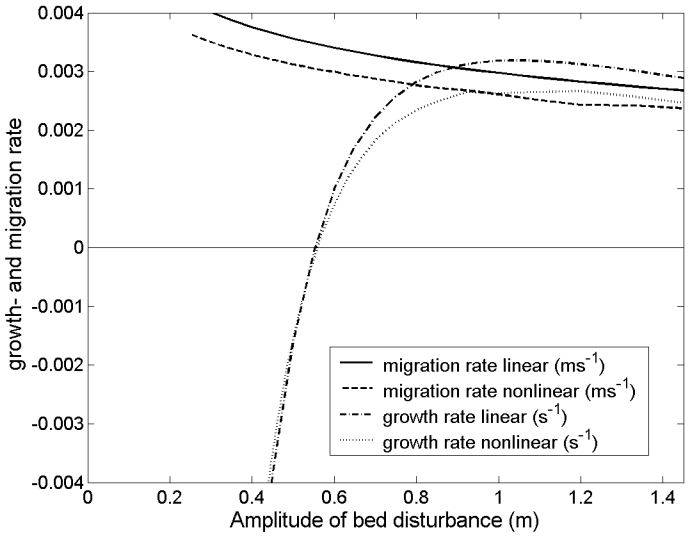

Figure 6. Stability plot showing the growth and migration rate of sinusoidal disturbances as a function of wave length of the disturbance, determined with a linear and nonlinear stability analysis.

4.2 *Imposing TRIangular Asymmetric Stoss-side ripples (TRIAS ripples)*

The experiments showed that some of the superimposed dunes grow out to be the crest of the dune upon which they were superimposed (i.e. dune IV in Fig. 4). Other superimposed dunes do not break down the underlying dune, but transport sediment to the dune crest. (e.g. dune II & III). The dune that grew out to become the crest of the underlying dune (i.e. dune IV) showed the presence of a developed angle of repose lee side, which seems the main difference with the dunes that did not break down the underlying dune. The superimposed dune that survived and broke down the underlying dune, resembles the feature that Venditti et al. (2005) describe as sand sheets.

The stability analysis presented in Section 4.1 showed that superimposed disturbances with short wavelengths will dissolve, because of their negative growth rate. However, if flow separation occurs behind the superimposed disturbances, all sediment

transported over its crest is deposited behind the crest. This assures that such disturbances do not dissolve/diffuse.

Based on these considerations, we superimposed a bed feature, called a TRIAS-ripple (i.e. TRIangular Asymmetric Stoss-side ripple). The shape of the superimposed TRIAS-ripples is based on five criteria (see also figure 7):

- Relatively small height with respect to the underlying dune
- Angle of repose lee side to assure flow separation behind the crest
- No net sediment accretion or erosion to assure sediment continuity
- Smooth connection to the existing bottom to prevent numerical difficulties
- Superimposed between the reattachment point of the upstream dune and the crest of the downstream dune to make sure it migrates over the upper half of the stoss side, as observed in experiments (compare figure 4)

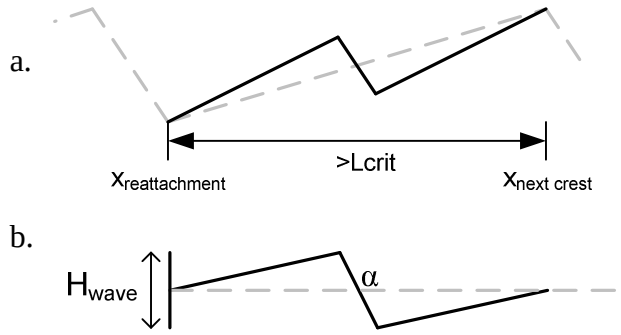

Figure 7. Schematisation of superimposed TRIAS-ripple
a. on top of a stoss side which exceeds the critical length.
b. explaining TRIAS-ripple height *Hwave* and lee side angle α.

A TRIAS-ripple is superimposed on the stoss side, such that the underlying stoss side is split in two. The TRIAS-ripple is superimposed as soon as the length of the underlying stoss side (i.e. the distance from the reattachment point to the downstream dune crest) exceeds a certain critical value L_{crit}. The value of L_{crit} is set such that the TRIAS-ripple has the minimum wavelength for which growth is perceived, based on the stability analysis (i.e. 0.5 *m*, leading to a value of L_{crit} of 1.0 *m*). For comparison, in the experiments superimposed TRIAS-ripples have been observed on dunes with dune lengths ranging from 1 *m* to 1.4 *m*. The TRIAS-ripple is created with a predetermined amplitude H_{wave} of 12 *mm* and an angle of repose α of -30º.

Figure 8 shows some model simulations in which TRIAS-ripples are superimposed as soon as the stoss side length exceeds $L_{crit.}$ The results show that the superimposed TRIAS-ripple starts to grow instantaneously until it reaches the crest of the underlying dune. When that happens it limits the sediment transport to the crest. The underlying crest slows down and dissolves. The flow separation zone of the superimposed TRIAS-ripple grows and overtakes the dune crest of the underlying dune. Apparently, a superimposed TRIAS-ripple has the ability to shift the dune crest of the underlying dune upstream, thereby limiting the dune length. If the superimposed TRIAS-ripple has overtaken the dune completely and the stoss side becomes too long again, the process repeats itself.

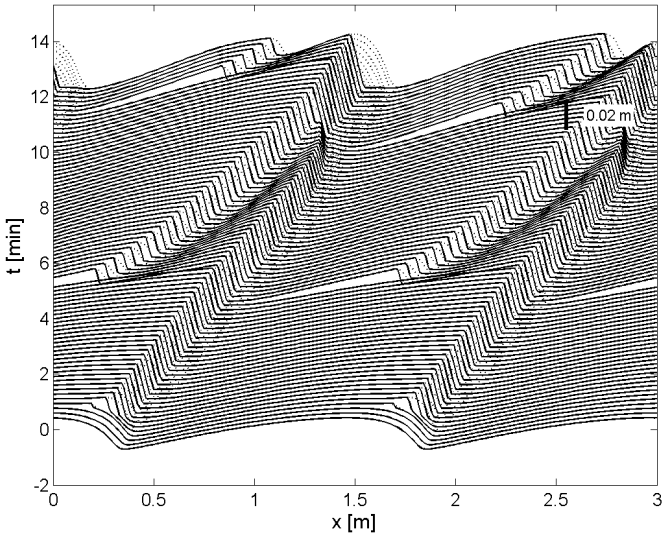

Figure 8. Model simulations, including superposition of TRIAS-ripples when the stoss side length exceeds L_{crit}.

5 MODEL VALIDATION

To validate the extended model, experiment T22 is simulated with the model (see Table 1 for values of the input parameters: initial water depth H_0, median grain size D_{50}, bed slope i_0 and specific discharge q). Figure 9 shows that, in contrast to simulations with the original model (compare Figure 2), both dune merging and dune splitting occur, leading to a limited dune length and thus to equilibrium dune dimensions.

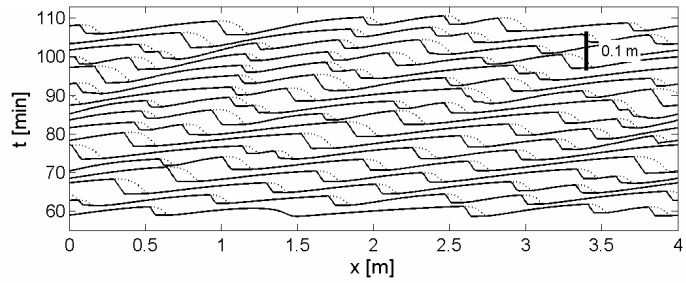

Figure 9. Simulations of extended model (including superposition of TRIAS-ripples) when dunes have reached a dynamic equilibrium with continuous merging and splitting of dunes.

A comparison between measured and calculated evolution of dune height and dune length is presented in Figure 10. In addition, equilibrium dune dimensions as observed in the measurements, and as predicted by the original model (without dune split-

ting) and by the extended model (including superposition of TRIAS-ripples) are presented in Table 3.

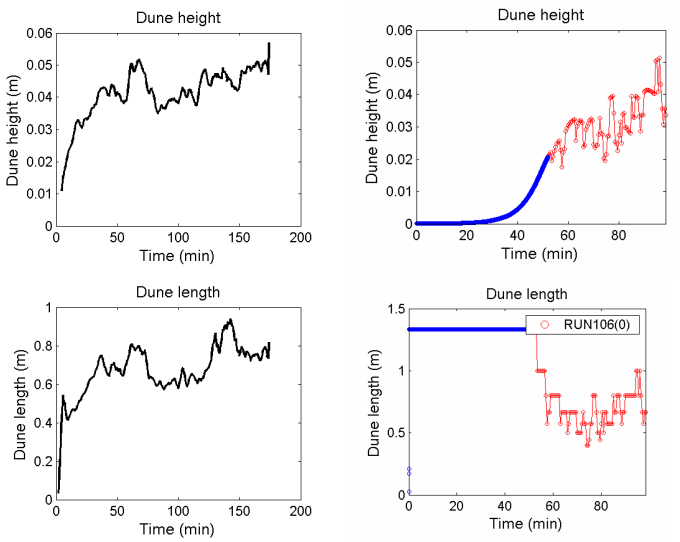

Figure 10. Evolution of dune height (upper panels) and dune length (lower panels) as observed in the experiments (left panels) and predicted by the extended model (right panels).

Figure 10 shows that in general the evolution pattern of dune height as predicted by the model is similar to the observed behaviour. Only the initial phase shows a clear difference: in the experiment dunes reach a height of about 0.01 *m* very quickly after the start of the experiment. Because of this short time, it is not known exactly how this initial evolution occurs. In the model, dune height grows very gradually in the beginning and it takes much longer to reach a height of 0.01 *m*. However, from that instance, dune height development in the model is very similar to the observed dune height evolution. Also, the initial development of simulated dune length is different from the observations. This is because in the model, all small wave lengths are damped very quickly (see the stability analysis in Section 4.1) and only the longer wave lengths start to grow, particularly the fastest growing mode, which has a length of about 1.3 *m* in this case. If flow separation starts to play a role and the stoss side behind the reattachment point exceeds the critical stoss side length L_{crit}, dune splitting occurs (due to the superposition of TRIAS-ripples) and dune length is reduced (see figure 7a).

Table 3 shows that the equilibrium dune height and dune length, as predicted by the extended model, are similar to the values observed in the measurements and much closer to the measurements than the predictions of the original model. Also the migration rate, the time to equilibrium and the final water depth are predicted rather well by the extended model and predictions are significantly improved, compared to the original model (see Table 3). The fact that the extended model yields better predictions of the final water depth than the original model is an indication that the hydraulic roughness due to the presence of dunes is better captured by the extended model (which agrees with the fact that dune dimensions are predicted better by this model).

Table 3. Comparison between measured and predicted parameters of dune evolution in equilibrium conditions.

Parameter	Measured (exp. T22)	Original model	Extended model
Dune height Δ (*m*)	0.05	0.146	0.04
Dune length λ (*m*)	0.75	4.0	0.7
Migration rate (*m/hr*)	4	3	4
Time to equilibrium (*min*)	55	180	65
Water depth *H* (*m*)	0.190	0.23	0.180

6 DISCUSSION & CONCLUSIONS

We included dune splitting in the dune development model of Paarlberg et al. (2006; subm.) by superposition of TRIAS-ripples as soon as the stoss side becomes longer than a certain critical value. This critical stoss side length is subject to discussion. The model results are sensitive to the value of the critical stoss side length. In this paper, this value is fixed and equal to the smallest wavelength that will be able to grow. This wave length is determined from a nonlinear stability analysis, carried out with the initial model settings (and thus the initial flow conditions). In future research, we will extend the model such that the critical stoss side length will be determined internally in the model, based on a stability analysis for the actual flow conditions.

In this paper we have addressed two research questions. First, we have investigated what the mechanism is behind dune splitting that results in limited growth of dune length. Based on knowledge from literature and new laboratory experiments performed at the University of Auckland, we conclude that random initiation of superimposed bed forms seems one of the main mechanisms for dune splitting. These small bed forms only grow if the stoss side of the underlying dune is sufficiently long. Moreover, dune splitting and therefore a reduction of dune length occurs particularly if the lee side of the superimposed bed form is so steep that flow separation occurs behind the superimposed bed form. Due to flow separation, all sediment that passes the dune crest stays in the flow separation zone, enabling the superimposed bed form to grow and migrate.

Next, we addressed the question of how to implement dune splitting in the dune development model of Paarlberg et al. (2006; subm.) and whether this leads to better predictions of dune dimensions. Based on the answer to the first research question, we implemented dune splitting by superposition of TRIAS-ripples (TRIangular Asymmetric Stoss side-ripples) on developing dunes as soon as the stoss sides of these dunes exceeds a certain critical length. This critical length is equal to the smallest length of a bottom disturbance that can grow in the system

under consideration, as determined from a nonlinear stability analysis. Based on observations from literature and from our own experiments the TRIAS-ripples are asymmetrically shaped with an angle of repose lee side, such that flow separation occurs behind them. The superposition of TRIAS-ripples leads to dune splitting and thus to a reduction in dune length.

Simulations with the extended model (including dune splitting) shows that predictions of equilibrium dune characteristics such as dune height, dune length, migration rate, time to equilibrium and final water depth are significantly improved compared to the original model.

ACKNOWLEDGEMENTS

This study is carried out as part of the project 'Dynamic roughness in rivers during floods', supported by the Technology Foundation STW, the applied science division of NWO and the technology programme of the Ministry of Economic Affairs (Project No. 06222). We are very grateful to STW for the grant to the second author to travel to New Zealand to carry out the experiments. Moreover, we would like to thank Prof. Stephen Coleman and Heide Friedrich from the University of Auckland, New Zealand, for making it possible to carry out experiments in their laboratory flume and for their help and support during the experiments.

REFERENCES

Allen, J.R.L. 1978. Computational methods for dune time-lag: Calculations using Stein's rule for dune height. *Sedimentary Geology* 20(3): 165-216.

Coleman. S.E., Zhang, M.H. & Clunie, T.M. 2005. Sediment-wave development in subcritical water flow. *J. Hydr. Eng.* 131(2): 106-111.

Coleman, S.E., & Melville, B. W. 1997. Ultrasonic measurement of sediment bed profiles. *Proc. 27th Congress of the Int. Ass. for Hydr. Res., San Francisco, U.S.A:* B221-B226.

Engelund, F. 1970. Instability of erodible beds. *Journal of Fluid Mechanics* 42: 225-244.

Fredsøe, J. 1974. On the development of dunes in erodible channels. *Journal of Fluid Mechanics* 64: 1-16.

Friedrich, H., Paarlberg, A.J. & Lansink, J. 2007. Evaluation of statistical properties of dune profiles. In C.M. Dohmen-Janssen & S.J.M.H. Hulscher (eds), *Proc. of the 5th IAHR Symposium on River, Coastal and Estuarine Morphodynamics RCEM 2007, Enschede, 17-21 Sept. 2007.* London: Taylor & Francis Group.

Giri, S. & Shimizu, Y. 2006. Computation of sand dune migration with free surface flow. *Water Resources Research* 42: W10422, doi: 10.1029/2005WR004588.

Jerolmack, D.J. & Mohrig, D. 2005. A unified model for subaqueous bed form dynamics. *Water Resources Research,* 41: W12421, doi:10.1029/2005WR004329.

Kennedy, J.F. 1963. The mechanics of dunes and antidunes in erodible-bed channels. *J. of Fluid. Mech.* 16: 521-544.

Leclair, S.F. 2002. Preservation of cross-strata due to migration of subaqueous dunes: an experimental investigation. *Sedimentology* 49: 1157 - 1180.

Nelson, J.M., Burman, A.R., Shimizu, Y., McLean, S.R., Shreve, R.L., & Schmeeckle, M. 2005. Computing flow and sediment transport over bedforms. In G. Parker & M. H. Garcia (eds), *Proc. of the 4th IAHR Symposium on River, Coastal and Estuarine Morphodynamics, Urbana, Illinois, USA,* Vol. 2: 861–872. London: Taylor & Francis Group.

Paarlberg, A.J., Dohmen-Janssen, C.M. Hulscher, S.J.M.H, Van den Berg, J. & Termes, A.P.P. 2006. Modelling morphodynamic evolution of river dunes. In Ferreira, Alves, Leal & Corsado (eds), *Proc. River Flow 2006:* 969-978. London: Taylor & Francis Group, ISBN 0-415-40815-6.

Paarlberg, A.J., Dohmen-Janssen, C.M., Hulscher, S.J.M.H. & Termes, P. 2007. A parameterization of flow separation over subaqueous dunes, *Water Resour. Res.*, 43, W12417, doi:10.1029/2006WR005425.

Paarlberg, A.J., Dohmen-Janssen, C.M., Hulscher, S.J.M.H & Termes, A.P.P. subm. Modelling river dune development using a parameterization of flow separation. *Submitted to J. of Geoph. Res – Earth Surface.*

Shimizu, Y. Schmeeckle, M.W. & Nelson, J.M. 2001. Direct numerical simulations of turbulence over two-dimensional dunes using CIP methods. *J. of Hydroscience and Hydraulic Eng.* 19(2): 85-92.

Tjerry, S. & Fredsoe, J. 2005. Calculation of dune morphology. *J. of Geoph. Res.-Earth Surface* 110 (F4), Art. No. F04013.

Van Rijn, L.C. 1984. Sediment transport part III: Bed forms and alluvial roughness. *J. of Hydr. Eng., ASCE,* 110 (12): 1733-1754.

Venditti J.G., Church, M.A. & Bennett, S.J. 2005. Morphodynamics of small-scale superposed sand waves over migrating dune bed forms. *Water Resources Research* W10423, doi: 10.1029/2004WR003461.

Yalin, M.S. 1964. Geometrical properties of sand waves. *J. Hydr. Div., ASCE,* 90(5).

Yamaguchi, S. & Izumi, N. 2002. Weakly nonlinear stability analysis of dune formation. *In Bousmar and Zech (eds.), Proc. River Flow 2002*: 843-850. Lisse: Swets and Zeitlinger, ISBN 90 5809 509 6.